Eur. Phys. J. A **12**, 269–277 (2001)

THE EUROPEAN PHYSICAL JOURNAL A

First measurement of β-decay properties of the proton drip-line nucleus ^{60}Ga*

C. Mazzocchi[1,2,a], Z. Janas[1,3], J. Döring[1], M. Axiotis[4], L. Batist[5], R. Borcea[1], D. Cano-Ott[6], E. Caurier[7], G. de Angelis[4], E. Farnea[4,10], A. Faßbender[1], A. Gadea[4,8], H. Grawe[1], A. Jungclaus[9], M. Kapica[1], R. Kirchner[1], J. Kurcewicz[1], S.M. Lenzi[10], T. Martínez[4,8], I. Mukha[1], E. Nácher[8], D.R. Napoli[4], E. Roeckl[1], B. Rubio[8], R. Schwengner[11], J.L. Tain[8], and C.A. Ur[10]

[1] Gesellschaft für Schwerionenforschung, Darmstadt, D-64291 Darmstadt, Germany
[2] Universitá degli Studi di Milano, I-20133 Milano, Italy
[3] Institute of Experimental Physics, University of Warsaw, PL-00681 Warsaw, Poland
[4] Laboratori Nazionali di Legnaro - INFN, I-35020 Legnaro, Italy
[5] St. Petersburg Nuclear Physics Institute, RU-188-350 Gatchina, Russia
[6] Department of Nuclear Fission, CIEMAT, E-28040 Madrid, Spain
[7] Institut de Recherches Subatomiques (IN2P3-CNRS-Université Louis Pasteur), F-67037 Strasbourg Cedex 2, France
[8] Instituto de Fisica Corpuscular, CSIC-Universidad de Valencia, E-46100 Burjassot-Valencia, Spain
[9] Departamento de Fisica Teórica, Universidad Autónoma de Madrid, E-28049 and Instituto Estructura de la Materia, CSIC, E-28006 Madrid, Spain
[10] Dipartimento di Fisica dell'Universitá di Padova and INFN, I-35131 Padova, Italy
[11] Forschungszentrum Rossendorf, D-01314 Dresden, Germany

Received: 4 September 2001 / Revised version: 23 October 2001
Communicated by J. Äystö

Abstract. By using the fusion-evaporation reaction ^{28}Si(^{36}Ar,p3n) and spectroscopy of β-delayed γ-rays and charged particles on mass-separated sources, β-decay properties of the neutron-deficient isotope ^{60}Ga were studied for the first time. The half-life of ^{60}Ga was determined to be 70(15) ms, and, based on $\beta\gamma\gamma$ coincidences, the isobaric-analogue state in ^{60}Zn was identified at 4851.9(7) keV. A semiempirical proton separation energy value of 40(70) keV was deduced for ^{60}Ga. The experimental results on half-life, mass excess, proton separation energy, and structure of the ^{60}Zn daughter states are discussed in comparison with various model predictions, including large-scale shell model calculations.

PACS. 21.10.-k Properties of nuclei; nuclear energy levels – 23.40.-s Beta decay; double beta decay; electron and muon capture – 21.60.Cs Shell model

1 Introduction

The remarkable progress in experimental and theoretical investigations of $N \sim Z$ nuclei, achieved in recent years, has been motivated by a multidisciplinary interest. The disciplines involved are i) nuclear-structure physics, in particular effects related to the occupation of identical orbits by neutrons and protons in the vicinity of the proton drip-line (see *e.g.* [1]), ii) fundamental physics, *e.g.*, tests of the standard model of weak interaction by precision measurements of superallowed $0^+ \rightarrow 0^+ \beta$-decays [2], and iii) astrophysics, concerning, *e.g.*, the electron capture (EC) cooling of supernovae [3] or the astrophysical rp-process [4]. A particularly interesting sample of $N \sim Z$ nuclei is the series of $N = Z-2$ ($T_Z = -1$) odd-odd nuclei in the pf shell. This series includes ^{40}Sc [5,6], ^{44}V [7–9], ^{48}Mn [10,11], ^{52}Co [8], and ^{56}Cu [12,13], as far as experimental knowledge of β-decay properties is concerned. The data on β-delayed emission of γ-rays, protons or α-particles, obtained for these nuclei, have yielded valuable contributions to the disciplines mentioned above. Furthermore, the observation of ^{60}Ga [14,15] and ^{64}As [14] in fragmentation reactions has given evidence that their ground states are probably bound or weakly unbound against proton emission. Correspondingly, β-decay is expected to be the dominant disintegration mode. However, these experiments did not yield any decay properties for ^{60}Ga and ^{64}As.

This paper reports on the first measurement of decay properties of ^{60}Ga. We shall begin by a general discussion of the decay properties of $T_Z = -1$ odd-odd nuclei in the pf shell and present then the experimental methods and results, followed by a discussion of model predictions and end with a summary and an outlook.

* This work is part of the Ph. D. thesis of C. Mazzocchi.

[a] e-mail: c.mazzocchi@gsi.de

Table 1. Beta-decay properties of $T_Z = -1$ odd-odd nuclei in the pf shell: spin and parity of the β-decaying state (I^π), half-life ($T_{1/2}$), electron-capture decay Q value ($Q_{\rm EC}$), excitation energy ($E_{\rm IAS}$) of the lowest-lying daughter state with $T = 1$ and an I^π assignment identical to that of the β-decaying state (isobaric-analogue state), proton and α separation energy in the daughter nucleus ($S_{\rm p}$, S_α), β-decay branching ratio for the transition populating the isobaric-analogue state ($b_\beta^{\rm IAS}$) and for transitions leading to the emission of protons and α-particles ($b_{\beta{\rm p}}$, $b_{\beta\alpha}$). The $Q_{\rm EC}$, $S_{\rm p}$ and S_α data stem from [17] whereas additional literature data were included for ^{40}Sc [5,6], ^{44}V [7–9], ^{48}Mn [10,11], ^{52g}Co [8], and ^{56}Cu [12,13].

Nucleus	I^π	$T_{1/2}$ (ms)	$Q_{\rm EC}$ (keV)	$E_{\rm IAS}$ (keV)	$b_\beta^{\rm IAS}$ (%)	$S_{\rm p}$ (keV)	$b_{\beta{\rm p}}$ (10^{-3})	S_α (keV)	$b_{\beta\alpha}$ (10^{-4})
^{40}Sc	4^-	182.3(7)	14320(4)	7658.23(5)	49.4(40)	8328.24(9)	4.4(7)	7040.6(4)	1.7(5)
^{44g}V	(2^+)	111(7)	13700(80)[a]	6606.4(5)	30.1(50)	8649.6(20)	–	5127.1(7)	[b]
^{44m}V	(6^+)	150(3)	14000(80)[a]	6848.84(22)	43.6(46)	8649.6(20)	–	5127.1(7)	–
^{48}Mn	4^+	158.1(22)	13607(22)	5792.4(6)	57.5(35)	8103(7)	2.80(37)	7694(8)	–
^{52g}Co	6^+	115(23)	14409(70)[a]	5655.37(51)	100	7381(12)	–	7939(13)	–
^{56}Cu	4^+	93(3)	15300(140)[a]	6431.7(7)	67.5(37)	7165(11)	4.0(12)	7995(15)	–

(a) Values estimated from systematic trends [17].
(b) Beta-delayed α emission observed, corresponding branching ratio unknown [7].

2 Decay properties of $T_Z = -1$ odd-odd nuclei in the pf shell

Before presenting the experimental results obtained for the ^{60}Ga decay, we want to inspect the decay properties of other $T_Z = -1$ odd-odd nuclei in the pf shell, which are listed in table 1. The following trends are observed when going from ^{40}Sc to ^{56}Cu, the two nuclei representing one-proton particle, one-neutron hole configurations with respect to the core nuclei ^{40}Ca and ^{56}Ni, respectively:

i) Except for the particularly high $Q_{\rm EC}$ value and energy ($E_{\rm IAS}$) of the isobaric-analogue state (IAS) of ^{40}Sc and ^{56}Cu, these energies show a smooth behaviour as a function of the mass number for the other three nuclei. Correspondingly, the superallowed transition to the IAS in the respective daughter nucleus represents a strong part (30% to 100%, see table 1) of the β intensity.
ii) Next to the superallowed transition, a sizeable fraction of the β intensity originates in the Gamow-Teller decay to the lowest-lying daughter level characterized by spin and parity values identical to those of the β-decaying state. The corresponding β intensities are 32(12)% for ^{44g}V [8], 56.4(4.6)% for ^{44m}V [8], 6.1(4.4)% for ^{48}Mn [10], $\leq$24% for ^{52g}Co [8], and 36(14)% for ^{56}Cu [12].
iii) The consequence of the features i) and ii) is that the half-lives do not show much variation (93 to 182 ms, see table 1), and that the γ-ray de-excitation of the primarily populated states in the daughter nuclei yield a strong $E2$ transition from the first excited 2^+ level to the 0^+ ground state.
iv) As the IAS is either bound or only weakly unbound against proton and α-decay, the emission of β-delayed protons (βp) or β-delayed α-particles ($\beta\alpha$) is a rare process (branching ratios of $1.7 \cdot 10^{-4}$ to $4.4 \cdot 10^{-3}$, see table 1), reflecting the low intensities of Gamow-Teller transitions to high-lying daughter states.

We assume an assignment of 2^+ for the ground state of ^{60}Ga in analogy to the mirror nucleus ^{60}Cu [16]. Furthermore, a value of $Q_{\rm EC} = 14183(111)$ keV was estimated in ref. [17]. Based on these properties, we expect the decay of ^{60}Ga to be characterised by a half-life of the order of 100 ms, by the occurence of β-delayed γ-rays ($\beta\gamma$), including the known [16] 1004.2(5) keV $2^+ \rightarrow 0^+$ transition, and by weak βp and/or $\beta\alpha$ intensities.

Previously the $I^\pi = 2^+$, $T = 1$ IAS in ^{60}Zn was measured at 4.8(1) MeV in a two-nucleon stripping reaction [18]. The IAS is bound against proton emission ($S_{\rm p} = 5121(11)$ keV [17]) but unbound against α emission by 2206(15) keV ($S_\alpha = 2708(15)$ keV [17]). Therefore, a weak $\beta\alpha$ line of 2.2 MeV might be expected in the ^{60}Ga decay.

3 Experimental methods

^{60}Ga nuclei were produced in ^{28}Si(^{36}Ar,p3n) fusion-evaporation reactions, induced by a 4.71 MeV · A, 85 particle-nA ^{36}Ar beam on a natural-silicon target. The targets, whose thickness ranged from 2.1 to 2.5 mg/cm^2 during the different measurements, were mounted close to the ion source of the GSI On-Line Mass Separator [19] in two separate experiments:

1) A FEBIAD-E [20] ion source was used, which yielded a mass-separated beam intensity of 1.8 ions/s for ^{60}Ga, based on the decay data obtained in this work. The $A = 60$ beam contained, however, strong isobaric contaminants of ^{60}Cu ($T_{1/2} = 23.7$ min [16]) and ^{60}Zn ($T_{1/2} = 2.38$ min [16]), produced by the ^{28}Si(^{36}Ar,3pn) and ^{28}Si(^{36}Ar, 2p2n) reactions, respectively.
2) A TIS [20,21] ion source was employed to strongly suppress the $A = 60$ contaminants compared to the values obtained during experiment 1. A suppression factor of 700 for the strongest contaminant ^{60}Cu and an even larger one for ^{60}Zn were reached, while the separation efficiency for ^{60}Ga was reduced by only a factor of 6 ($\sim$ 5% with TIS compared to $\sim$ 30% with FEBIAD) because of the lower efficiency of thermoionization.

In both experiments, the evaporation residues were stopped in a 0.1 mm thick catcher of sinter-graphite mounted inside the ion source and, after release from the catcher and ionization, extracted as a 55 keV beam of singly charged ions. For studying $\beta\gamma$ properties of ^{60}Ga, the mass-separated $A = 60$ beam was implanted in a movable tape remaining at rest for preset implantation periods during which the grow-in of the activity was measured by means of a $\beta\gamma$ detector array. Subsequently, the radioactive sources were removed from this position. In experiment 1, which lasted 13 h, the implantation interval amounted to 0.8 s in order to suppress the long-lived isobaric contaminants. In experiment 2, longer implantation intervals of 4 s and 12 s were chosen for measuring times of 12.8 and 9 h, respectively.

The $\beta\gamma$ set-up consisted of a plastic scintillator for positron detection, and two composite germanium (Ge) detectors of Clover type [22] and Cluster type [23] during experiment 1. For experiment 2, two additional detectors with a relative efficiency of 70% were included in the detector set-up. The efficiency of the plastic scintillator was estimated to be about 83% by comparing the number of the γ-rays observed as β-gated and singles events. The energies of the γ transitions, observed in the Ge detectors, were determined by using the known energies of the isobaric contaminants ^{60}Cu and ^{60}Zn [16], as well as standard calibration sources. The latter were also used to establish the energy-dependent efficiency. The photopeak efficiency of the Ge detector array amounted to about 2.8% [13] and 4.3% for experiment 1 and 2 respectively, for 1.33 MeV γ-rays if signals from individual Ge crystals were accumulated (single-hit mode). Summing the signals from neighbouring Ge crystals (add-back mode) improved the efficiency only by about 20%.

The search for βp and $\beta\alpha$ activities, was performed at another beam line of the On-Line Mass Separator during both experiments. The $A = 60$ beam was directed during consecutive time intervals to two 29 μg/cm^2 thick carbon foils which were each viewed by a telescope (telescopes A and B). Each of them covered 34% of 4π sr, and consisted of two silicon surface barrier detectors for recording energy loss (ΔE) and residual energy (E) of the β-delayed particles. The thicknesses and areas of the detectors were 20.1 μm, 450 mm^2 and 500 μm, 1200 mm^2 for the telescope A, and 22.5 μm, 450 mm^2 and 500 μm, 1200 mm^2 for the telescope B. The energy calibration of the ΔE and E detectors was achieved by using ^{148}Gd, ^{241}Am, ^{239}Pu and ^{244}Cm α sources. The energy resolution (FWHM) obtained for 3184 keV α-particles in the ΔE and E detectors amounted to about 100 and 50 keV, respectively, for the telescope A, and about 90 and 60 keV, respectively, for the telescope B. The combined action of the ΔE and E detectors led to an effective energy resolution (FWHM) of about 90 and 80 keV for the telescope A and B, respectively, for 3 MeV protons. Due to summation with positron (energy loss) signals, the response function of the telescopes to β-delayed particles was asymmetric, with a 34% high-energy tail.

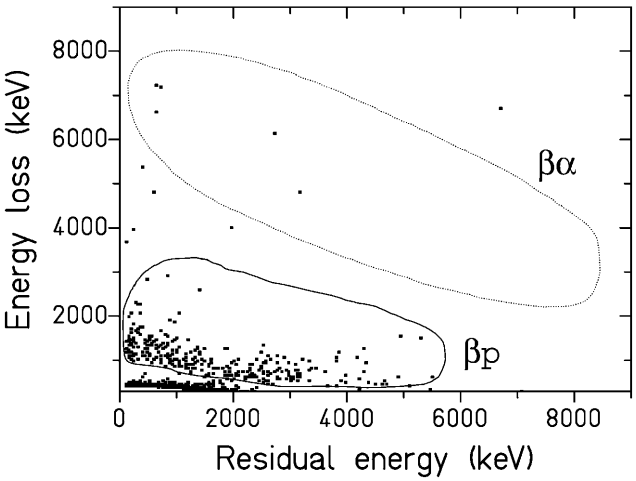

Fig. 1. Scatter plot of energy loss *versus* residual energy events recorded for $A = 60$ in telescope B during experiment 1. The areas used for selecting β-delayed protons and α-particles are marked by "βp" and "$\beta\alpha$".

The distinction between positrons, protons and α-particles was accomplished on the basis of $\Delta E - E$ scatter plots. An example of data taken by means of telescope B is displayed in fig. 1. For telescope A a similar identification plot was obtained, the difference being due to the different thicknesses of the two ΔE detectors. By choosing selected areas on these plots (see fig. 1), energy spectra of β-delayed particles were obtained by summation of coincident ΔE and E signals, and grow-in-decay time spectra of summed ΔE and E events were generated as a function of the time elapsed within the implantation intervals. The areas for identifying $\beta\alpha$ events were verified in a separate on-line measurement of mass-separated ^{114}Cs which has well-known β-delayed particle properties [24]. Two different implantation intervals were chosen, *i.e.* 1.0 and 0.4 s, with total measurement times of about 10 h for each interval. While events from both telescopes were added to deduce the energy spectra, the time analysis was based on the data accumulated by means of the telescope B only. The latter restriction was imposed as occasional delays occurred when the beam was deflected to the carbon foil in front of telescope A.

4 Experimental results

4.1 Assignment of β-delayed radiation to the ^{60}Ga decay

For assigning experimental $\beta\gamma$ and βp data to the decay of the ^{60}Ga ground state, we used the following arguments:

- the measurement was performed by using $A = 60$ sources;
- a ^{60}Ge assignment is excluded due to the much lower cross-section expected [25] for the 4n reaction channel with respect to the p3n channel;

– gallium is the only element in question with reasonable thermoionization efficiency, and the decrease of the βp events observed between the FEBIAD and the TIS ion sources (experiments 1 and 2) is in agreement with that expected from the respective efficiencies of ionization (see sect. 3);

4.2 Beta-delayed γ-ray emission

Figure 2 shows part of the $\beta\gamma$ data accumulated as the sum of β-coincident single-hit events from experiment 2. Three γ lines can clearly be observed, *i.e.* the known 1004 keV line corresponding to the $2^+ \rightarrow 0^+$ transition in the daughter nucleus ^{60}Zn, the 826 keV line of ^{60}Cu [16], and the 834 keV line of ^{72}As [26]. The latter activity represents a long-lived contamination of the transport tape from a previous $A = 72$ measurement. Moreover, a 3848 keV γ-ray has been identified, which shows an unambiguous coincidence relationship with the 1004 keV line (see fig. 3 and table 2). On the basis of these experimental data, we assign the 3848–1004 keV cascade to the de-excitation of the $I^\pi = 2^+$, $T = 1$ IAS in ^{60}Zn. This consideration positions the IAS at 4851.9(5) keV, as displayed in fig. 4 and table 2.

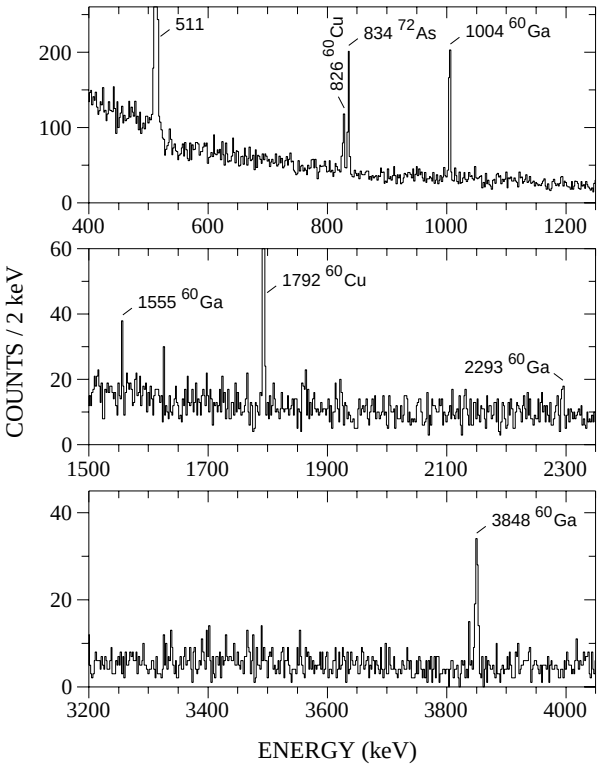

Fig. 2. Sections of the γ-ray spectrum measured in single-hit mode for $A = 60$. Energy intervals of 400–1250 keV, 1500–2350 keV and 3200–4050 keV of the β-coincident γ spectrum, obtained in experiment 2, are shown. The γ lines are marked by their energies in keV.

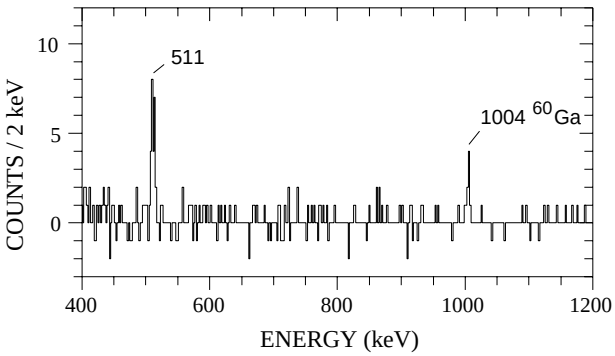

Fig. 3. Low-energy part of the γ spectrum taken in coincidence with positrons and 3848.3 keV γ-rays. It represents the sum of the data from experiments 1 and 2. The γ lines are marked by their energies in keV.

Table 2. Energies of the levels ($E_{\rm level}$) and γ lines (E_γ) in ^{60}Zn following the β-decay of ^{60}Ga, relative intensity (I_γ) of the lines and apparent β feeding (b_β) of the levels.

$E_{\rm level}$ (keV)	E_γ (keV)	Coincident γ transitions (keV)	I_γ (%)	b_β (%)
1003.7(2)	1003.7(2)	511, 3848.3	100(17)	27(19)
2558.7(5)	1554.9(6)	–	12(5)	13(8)
	2559.0(8)	–	13(5)	
4851.9(5)	2293.0(10)	–	10(5)	60(12)
	3848.3(7)	511, 1003.7	57(13)	

Moreover, an inspection of the β-gated γ-ray spectrum (see fig. 2) revealed three additional γ lines at energies of 1555, 2293 and 2559 keV (see table 2). These transitions are considered to be part of the $\beta\gamma$-decay branch of the ^{60}Ga ground state, despite the fact that rigorous $\beta\gamma\gamma$ coincidences have not been observed due to their weak γ-ray intensities. The assignment to the ^{60}Ga decay is based on the following reasons:

– the energies of the 2559 and 2293 keV lines match very well the IAS energy, and the energy of the new level at 2559 keV agrees with the sum of the 1555 keV line with the known 1004 keV transition (see fig. 4);
– all three γ lines do not belong to the well-known contaminants ^{60}Cu [16] and ^{72}As [26], nor constitute summation and/or escape peaks from known $\beta\gamma$ transitions of ^{60}Ga, ^{60}Cu and ^{72}As.

The new level at 2559 keV may correspond to the 2.65(20) MeV level observed in an early (^{3}He,n) measurement [27]. Furthermore, an indirect hint for such a level can be obtained from another (^{3}He,nγ) reaction study, where the neutron-gated γ-ray spectrum (see fig. 7 in ref. [28]) shows several unidentified γ-rays in an energy range close to our 1555 keV transition. The β feeding constrains spin parity of this state to $(1–3)^+$, whereas the ground state γ-ray branch excludes 3^+. We tentatively as-

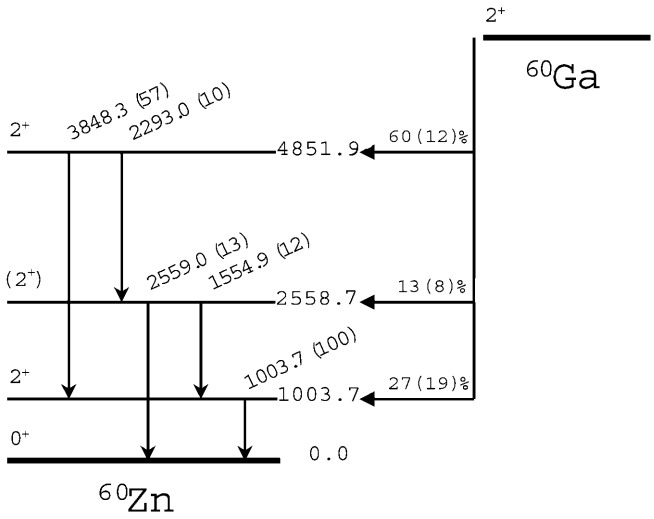

Fig. 4. Decay scheme of ^{60}Zn following the β-decay of ^{60}Ga obtained in this work.

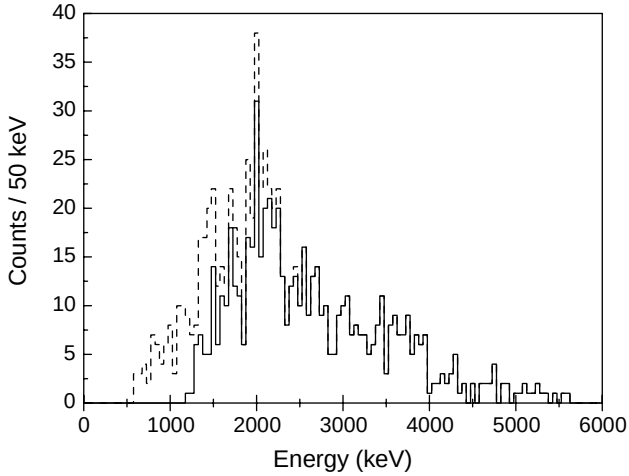

Fig. 5. Energy spectrum of βp events registered by the two telescopes and assigned to the decay of ^{60}Ga. The solid-line histogram shows events obtained by $\Delta E - E$ coincidence, while the dashed-line spectrum is the sum of the events accumulated in ΔE detector in anticoincidence with signals from the E detector and those accumulated in coincidence, in the energy range 600–2400 keV.

sign $I^\pi = (2^+)$ to the state at 2259 keV on the following grounds:

- in none of the even-even zinc isotopes, $N = 30$ isotones and $N = Z$ nuclei, a 1^+ state is known to exist below the 2_2^+ state;
- in the ^{44}V β^+/EC-decay, which is identical to that of ^{60}Ga with respect to half-life, $Q_{\rm EC}$ value, parent spin (see table 1 and ref. [8]), and doubly magic + 2p2n structure of the daughter nucleus, exclusively $I^\pi = 2^+$ states are fed.

The experimental γ-ray intensities yield the apparent β feedings listed in table 2. The half-life analysis of the five γ lines and of the 511 keV γ-ray was limited by poor statistical quality, but yielded agreement with the βp result discussed below.

4.3 Beta-delayed proton emission

4.3.1 Selection and energy spectrum of β-delayed protons

We selected βp events by using the "βp area" of the $\Delta E - E$ scatter plot, as indicated in fig. 1. By applying this procedure to the data obtained from the telescopes A and B, the βp energy spectrum was obtained as shown in fig. 5 for experiment 1. This spectrum contains 325 and 288 events in telescope A and B, respectively, hence a total of 613. It extends from 1500 to 5500 keV, which corresponds, assuming $S_{\rm p} = 5121(11)$ keV [17] and proton emission to the ground state of ^{59}Cu, to a range of ^{60}Zn excitation energies from 6600 to 10600 keV.

The βp-energy spectrum shown in fig. 5 is assigned to the decay of ^{60}Ga on the basis of the arguments given in subsect. 4.1, and taking into account that

- the "βp window" $Q_{\rm EC} - S_{\rm p}$ of ^{60}Ga is estimated [17] to be 9060(180) keV, whereas it is known [17] to be negative for ^{60}Cu and ^{60}Zn and estimated [17] to be considerably smaller for ^{60}Ge;
- the experimental half-life, discussed in subsubsect. 4.3.2, is considerably shorter than those known [16] for the isobaric contaminants ^{60}Cu ($T_{1/2} = 23.7$ min) and ^{60}Zn ($T_{1/2} = 2.38$ min).

The βp spectrum, displayed in fig. 5 as a solid-line histogram, is influenced in its low-energy part by an experimental threshold. This is due to the fact that protons up to energies of 1200 to 2400 keV are completely stopped in the ΔE detectors, and are thus not recorded as $\Delta E - E$ coincidence events. This range of energies is related to the variation of the effective thicknesses of the ΔE detectors due to different angles of incidence, and to a lesser extent from the difference in their thicknesses. The net effect is that the spectrum displayed in fig. 5 by the solid-line histogram suffers from a low-energy threshold that sets in at 1200 keV and disappears at 2400 keV.

For further investigating the effect of the threshold introduced by the ΔE detectors, we inspect the energy spectrum accumulated by using signals from these detectors in anticoincidence with signals from the E detectors. The resulting spectrum in the energy range from 600 to 2400 keV is also shown in fig. 5. The 189 events, occurring in this energy range, with weak indication for peak structures around 1.5, 1.8 and 2.0 MeV, can be due either to external background or $A = 60$ positron activity, or to βp or $\beta\alpha$ emission. Unfortunately, we are unable to make a firm distinction between such contributions. However, as will be discussed in sect. 5, there are reasons to assign these low-energy events to βp rather than $\beta\alpha$ emission. Correspondingly, the total number of 613 βp events observed in $\Delta E - E$ coincidence has to be increased by 189, *i.e.* by 31%, if contributions from external background, positron and $\beta\alpha$ emission, are neglected (see subsubsect. 4.3.2).

4.3.2 Beta decay half-life

In order to determine the half-life of ^{60}Ga, we used βp events accumulated by means of telescope B and obtained by $\Delta E - E$ coincidences during experiment 1. The resulting data are plotted as a function of the time elapsed within the implantation intervals in fig. 6. A total of 147 and 141 events were accumulated for the implantation cycles of 1.0 and 0.4 s, respectively. By assuming a one-component exponential function for a least-squares fit of the experimental grow-in/decay characteristics, we obtained half-life values of 80(26) and 65(18) ms, respectively, corresponding to a mean value of 70(15) ms. We adopt this as the experimental β-decay half-life of ^{60}Ga.

An analysis of the time dependence of the 113 βp events that were recorded by operating the telescope B in ΔE anticoincidence mode (see subsubsect. 4.3.1), yielded half-life values of 250(80) and 120(30) ms for the implantation periods of 1.0 and 0.4 s, respectively. In view of the contributions from external background and from positrons which stem mostly from the longer-lived isobaric contaminants ^{60}Zn and ^{60}Cu, it is not surprising that these half-life results are somewhat larger than the value of 70(15) ms deduced from $\Delta E - E$ coincident events.

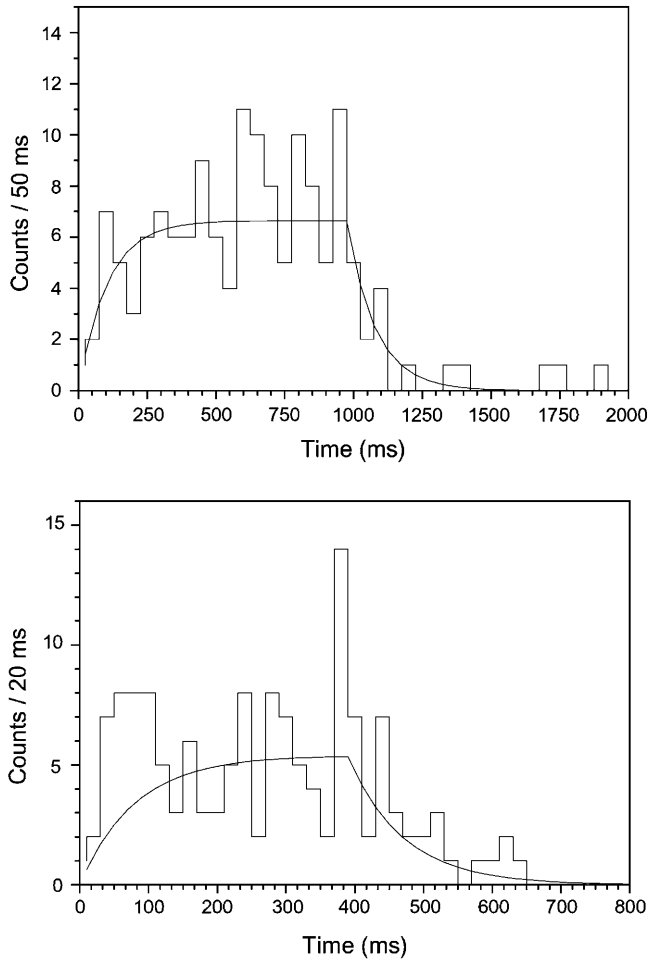

Fig. 6. Time dependence measured by means of telescope B for grow-in and decay of the βp activity. The implantation period amounted to 1 s (upper panel) and 0.4 s (lower panel).

4.3.3 Branching ratio for β-delayed proton emission

Experiment 2 allowed us to determine the branching ratio for βp emission ($b_{\beta \mathrm{p}}$). We observed 30 βp events during 5 h, and an intensity of 268 counts for the 1004 keV line during 12.8 h. By assuming the latter transition to have an intensity of 89% per ^{60}Ga decay (see fig. 4 and table 2), and by taking the proton and γ detection efficiencies as well as the incomplete saturation of the ^{60}Ga activity in the case of the γ measurement into account, we obtained a $b_{\beta \mathrm{p}}$ value of $(1.6 \pm 0.7)\%$. This estimate takes the 31% contribution of low-energy βp events into account, and includes also a systematic uncertainty of the same order of magnitude due to the problem of background subtraction (see subsubsect. 4.3.1).

4.4 Beta-delayed α emission

In the $\Delta E - E$ scatter plot displayed in fig. 1 one can identify five events that are candidates for $\beta\alpha$ emission. Together with the four $\beta\alpha$ candidate events observed in the corresponding $\Delta E - E$ area of telescope A, this corresponds to a total of nine $\beta\alpha$ candidate events. Their energies range from 7.3 to 8.9 MeV. The corresponding range of excitation energies in ^{60}Zn is 10.0 to 11.6 MeV if α emission to the ground state of ^{56}Ni is assumed. This $\beta\alpha$ rate corresponds to a ratio of 70(43) between the βp and $\beta\alpha$ intensities, and, together with the $b_{\beta \mathrm{p}}$ value mentioned in subsubsect. 4.3.3, to an upper limit for the $\beta\alpha$ branching ratio of $2.3(2.0) \cdot 10^{-4}$. We shall return to the question of additional low-energy $\beta\alpha$ events in sect. 5.

5 Discussion

5.1 Beta-delayed γ-ray emission

The excitation energy of 4851.9 keV, determined in this work for the 2^+, $T = 1$ IAS in ^{60}Zn, is in agreement with the value of 4.8(1) MeV found earlier [18], whereas we disagree with the "probable" assignment [16] of the IAS to the 4913.5(10) keV state. By using the semiempirical value of $Q_{\mathrm{EC}} = 14180(60)$ keV (see subsect. 5.3) for ^{60}Ga and the apparent β feeding discussed in subsect. 4.2, we estimated the sum of the Fermi and Gamow-Teller strengths to be 1.8(5) for the IAS and 0.12(8) for the 2559 keV state and 0.13(10) for the 1004 keV state. Considering the uncertainty, the value of the experimental β strength for the IAS is in agreement with the theoretical value of 2.0 for a pure Fermi transition, indicating that if part of the β-delayed γ-rays remained unobserved in the experiment, this will be only a minor fraction.

5.2 Comparison of low-lying states of ^{60}Zn and ^{62}Zn with shell-model predictions

The excitation energy of the newly assigned (2_2^+) state in ^{60}Zn is higher by about 400 keV than that of the corresponding level in neighbouring ($A = 62$–66) even-even zinc isotopes. In order to interpret this unusual phenomenon, we compare in fig. 7 the experimental energies of the 2_1^+, 4_1^+ and 2_2^+ states in ^{60}Zn and ^{62}Zn with shell model predictions. For the latter purpose, we have chosen the KB3G [29] interaction (see [13] for a recent example of using various interactions for calculating the β-decay properties of ^{56}Cu), and performed a large-scale calculation by using the code ANTOINE [30]. The truncation level t of the calculation, given as abscissa in fig. 7, identifies the maximum number of nucleons which are excited from the $f_{7/2}$ orbital to other pf shell orbitals. At $t = 6$, $400 \cdot 10^6$ and $525 \cdot 10^6$ basis states are used for ^{60}Zn and ^{62}Zn, respectively.

The trend of the levels with increasing number of particle-hole (ph) excitations indicates that the shell-model calculation has converged with $t = 6$. This is also born out by the fact that for the ^{60}Zn ground state, which can be calculated untruncated ($2.3 \cdot 10^9$ basis states), the

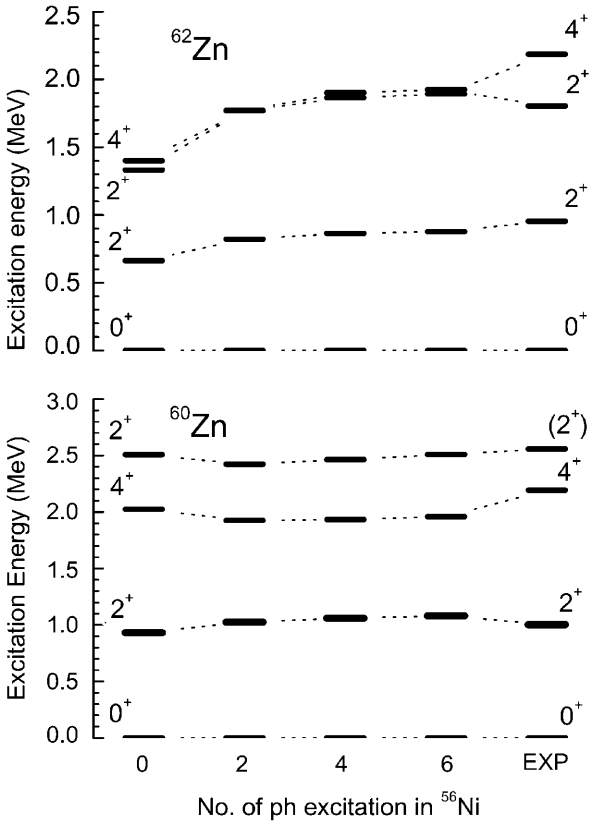

Fig. 7. Excitation energies of the 2_1^+, 4_1^+ and 2_2^+ states in ^{60}Zn and ^{62}Zn: experimental values are compared with shell-model predictions given as a function of the number of particle-hole excitations taken into account (or truncation level t). For clarity only even t values are shown.

$t = 6$ truncation level results only in a 25 keV deficiency in the binding energy. The $I^\pi = 2^+$ states are nicely reproduced, especially the step in excitation energy of the 2_2^+ level from ^{62}Zn (and the heavier isotopes) to ^{60}Zn. The 4^+ state in ^{60}Zn seems to be slightly overbound and it is not clear whether this is due to a deficiency of the interaction, or to the neglect of the $g_{9/2}$ orbital.

As for the nature of the discontinuity of the 2_2^+ state, it is interesting to note that an identical effect is observed in ^{20,22}Ne. The nuclei ^{60,62}Zn with respect to the doubly magic ^{56}Ni are the pair of nuclei corresponding to ^{20,22}Ne with respect to ^{16}O. It has been pointed out earlier [31], that the $f_{5/2}$, $p_{1/2}$, $p_{3/2}$ orbitals correspond to the $d_{5/2}$, $s_{1/2}$, $d_{3/2}$ orbitals in a pseudo-spin scheme. It was shown a long time ago [32] and studied systematically recently [33] that $SU(3)$ provides a viable truncation scheme to reproduce the trend in ^{20,22}Ne. Especially the occurrence of a low-lying 2_2^+ state in ^{20}Ne, which is assigned to the γ vibrational band, is nicely reproduced in the schematic calculation of ref. [32] as a consequence of $SU(3)$ symmetry in contrast to ^{22}Ne. Therefore, we conclude that the observed discontinuity in ^{60,62}Zn is of similar microscopic origin as in ^{20,22}Ne. It is intriguing to infer from the absence of this $2_{1,2}^+$ behaviour in the ^{44,46}Ti pair of isotopes above the doubly magic ^{40}Ca, situated in a pure $f_{7/2}$ shell, a supportive argument for the $SU(3)$ structure above ^{16}O and ^{56}Ni. It should be noted, however, that large-scale and Monte Carlo shell model studies have shown that low-lying states in ^{44,46}Ti are strongly distorted by ^{40}Ca core excitations [34,35], as known since long from experiment.

5.3 Masses and mass differences

Coulomb-energy systematics [26] allow us to determine the energy difference between the 2^+, $T = 1$ ground state of ^{60}Ga and the 2^+, $T = 1$ IAS in ^{60}Zn to be 9324(60) keV. The uncertainty of this semiempirical value was obtained as a mean-square deviation between experimentally known 2^+, $T = 1$ Coulomb displacement energies of $A =$ 50–60 nuclei and the corresponding prediction according to [26]. This result, together with the excitation energy of 4851.9(5) keV of the IAS yields a semiempirical Q_{EC} value of 14180(60) keV for ^{60}Ga. Furthermore, by using this result and the known mass excess values of $-54183(11)$ keV for ^{60}Zn and $-47260(40)$ keV for ^{59}Zn [17], we deduced the semiempirical results of $-40010(60)$ keV for the mass excess of ^{60}Ga and 40(70) keV for its S_{p} value. As the latter is compatible with zero, ^{60}Ga can indeed be called a proton drip-line nucleus.

The new experimental information that has been gained on the ^{60}Ga decay is confronted in table 3 with theoretical predictions. The semiempirical mass and mass difference data from this work agree with the corresponding values extrapolated from systematic trends [17] or determined by calculating Coulomb-energy differences between mirror nuclei on the basis of the shell model [36,37]. The macroscopic-microscopic model, based on the finite-range droplet model and the folded-Yukawa single-particle potential, "underbinds" ^{60}Ga, as can be seen from the less

Table 3. Experimental and theoretical data on Q_{EC}, mass excess, S_p and $T_{1/2}$ values of ^{60}Ga.

	This work	Predicted	Ref.
Q_{EC} (keV)	14180(60)	14183(111)	[17]
		14130(67)	[36]
		14570	[38]
Mass excess (keV)	−40010(60)	−40000(110)	[17]
		−40050(66)	[36]
		−39200	[38]
S_p (keV)	40(70)	30(150)	[17]
		80(77)	[36]
		28(19)	[37]
		−490	[38]
		−260	[39]
$T_{1/2}$ (ms)	70(15)	59.2	[38]
		48.5–73.0[(a)]	[40]
		> 0.0012	[17]

(a) Range of values due to different mass predictions.

negative mass excess and the negative S_p value [38]. The same is true, even though to a lesser extent, for the predictions obtained by using a relativistic Hartree-Bogoliubov model [39]. The half-life of ^{60}Ga agrees with the values predicted by the macroscopic-microscopic model [38] and the QRPA model [40].

5.4 Implications for the rp-process

The S_p values of neutron-deficient gallium isotopes are of crucial importance for the rp-process as they determine at which zinc isotope i) a captured proton is not removed right away by strong photodisintegration of the weakly proton-bound gallium isotone and ii) the rp-process can proceed to heavier elements via fast proton captures. Of special importance is the question to which degree the β-decay of the potential long-lived waiting point nucleus ^{60}Zn can be bypassed by proton captures on ^{59}Zn or ^{60}Zn. This depends sensitively on the S_p values of ^{60}Ga and ^{61}Ga. Recent calculations [41], which assumed an S_p value of 30(150) keV [17] for ^{60}Ga in agreement with the result obtained in this work, have shown that only a small fraction of 10^{-4} [42] of the rp-process flow runs through ^{60}Ga, while its dominant part involves the β-decay of ^{59}Zn. This is due to the small S_p value of ^{60}Ga. Furthermore, when considering the neighbouring zinc isotope ^{60}Zn as a candidate for an rp-process waiting point, one has to take into account that its effective half-life is supposed to be strongly reduced due to proton capture [42].

5.5 Beta-delayed particle emission

Considerations of spin and parity of the states involved (see subsect. 4.3), and of the selection rules for $\beta\gamma$, βp and $\beta\alpha$-decay, allow us to restrict the ^{60}Zn states that contribute to α and proton emission. From the 1^+, 2^+ and 3^+ states in ^{60}Zn, populated by allowed β-decay of ^{60}Ga, only the 2^+ levels can emit α-particles. The angular momentum carried by the emitted particle has to be $l = 2$ for $\beta\alpha$ and $l = 1$ for βp emission. WKB calculations performed for 0.9 MeV protons and 3.3 MeV α-particles, emitted from a ^{60}Zn level with an excitation energy of about 6 MeV, show that the probability to observe $\beta\alpha$ is several orders of magnitude smaller than for βp. Taking into account the observation of less than 10 "candidate" $\beta\alpha$ events observed at an energy of 1 MeV (see subsect. 4.4), the observation of $\beta\alpha$ from the ^{60}Ga decay was evidently beyond the sensitivity of our measurement. According to the angular-momentum selection rules mentioned above, $l = 2$ α-particles could be emitted also from the IAS. The corresponding α line, which would have an energy of 2.0 MeV, was not unambiguously observed in the ΔE spectra taken in anticoincidence with the E detectors, except for a weak indication based on a few events (see fig. 5). This is not surprising as the α-decay of the IAS is forbidden due to isospin selection rules.

6 Summary and outlook

By combining heavy-ion–induced fusion-evaporation reactions with on-line mass separation, we succeeded to study the β-decay of the $T_Z = -1$ odd-odd nucleus ^{60}Ga for the first time. Its half-life was measured to be 70(15) ms, and information has been gained on its βp and $\beta\gamma$ properties, as well as on the Q_{EC}, the mass excess and the S_p value of ^{60}Ga. The semiempirical estimate of 40(70) keV for the S_p value indicates that ^{60}Ga can indeed be considered to lie right at the proton drip-line. The half-life value obtained in this work agrees with that reported [43] at a recent conference.

For other members of the $T_Z = -1$ odd-odd nuclei, such as ^{44g}V [8], ^{48}Mn [10] and ^{52g}Co [8], experimental β-decay data were used to test predictions for excitation energies in the daughter nuclei and Gamow-Teller strengths, obtained by large-scale shell model calculations. Such a comparison is of interest for probing the assumptions made in developing the interaction used in the calculation, which is also relevant to astrophysical problems related to the rp-process or the EC cooling of supernovae. To reach this goal, however, a considerable increase of the quality of the ^{60}Ga data is needed, which involves further experimental improvements.

The relative positions of the $2^+_{1,2}$ states in ^{60,62}Zn show a close resemblance to ^{20,22}Ne, which can be traced back to an equivalent microscopic structure in a pseudo-$SU(3)$ scheme. Whether this opens the possibility for a viable truncation scheme in regions where untruncated large-scale shell model calculations are impossible, as *e.g.*, beyond ^{100}Sn, is still an open question. The abundantly available low- and high-spin data along the $N = Z$ line beyond ^{56}Ni await a quantitative theoretical analysis in terms of pseudo-$SU(3)$ in comparison to a full shell model calculation.

The authors would like to thank K. Burkard and W. Hüller for their help in developing and operating the GSI On-Line Mass Separator. Enlightening discussions with H. Schatz are gratefully acknowledged. This work was supported in part by the Polish Committee of Scientific Research, in particular under Grant No. KBN 2 P03B 086 17, by the Programme for Scientific Technical Collaboration (WTZ) under Projects No. POL 99/009 and RUS 98/672, and by the European Community under Contracts No. ERBFMGECT950083 and HPRI-CT-1999-00001.

References

1. E. Roeckl, in *Proceedings of the Shell Model 2000 Symposium, Tokyo*, edited by T. Otsuka, to be published in Nucl. Phys. A.
2. I.S. Towner, J.C. Hardy, in *Symmetries and Fundamental Interactions*, edited by E.M. Henley and H.C. Haxton (World Scientific, Singapore, 1995) p. 183.
3. K. Langanke *et al.*, Nucl. Phys. A **673**, 481 (2000).
4. H. Schatz *et al.*, Phys. Rep. **294**, 167 (1998).
5. J. Honkanen *et al.*, Nucl. Phys. A **380**, 410 (1982).
6. P.M. Endt, Nucl. Phys. A **521**, 1 (1990); **529**, 763 (1991) (Errata I); **564**, 609 (1993) (Errata II).
7. J. Cerny *et al.*, Phys. Lett. B **37**, 380 (1971).
8. E. Hagberg *et al.*, Nucl. Phys. A **613**, 183 (1997).
9. J.A. Cameron, B. Singh, Nucl. Data Sheets **88**, 299 (1999).
10. J. Szerypo *et al.*, Nucl. Phys. A **528**, 203 (1991).
11. T.W. Burrows, Nucl. Data Sheets **68**, 1 (1993).
12. M. Ramdhane *et al.*, Phys. Lett. B **432**, 22 (1998).
13. R. Borcea *et al.*, Nucl. Phys. A **695** (2001) 17; R. Borcea, Ph. D. Thesis, University of Bucarest, 2001.
14. B. Blank *et al.*, Phys. Rev. Lett. **74**, 4611 (1995).
15. R. Pfaff *et al.*, Phys. Rev. C **53**, 1753 (1996).
16. M.M. King, Nucl. Data Sheets **69**, 1 (1993).
17. G. Audi *et al.*, Nucl. Phys. A **624**, 1 (1997).
18. F. Pougheon *et al.*, Nucl. Phys. A **193**, 305 (1972).
19. K. Schmidt *et al.*, in *Proceedings of the 5th International Conference on Radioactive Nuclear Beams (RNB5), Divonne, April 2000*, edited by U. Koester, Nucl. Phys. A, in print.
20. R. Kirchner *et al.*, Nucl. Instrum. Methods **186**, 295 (1981).
21. R. Kirchner, Nucl. Instrum. Methods in Phys. Res. A **292**, 203 (1990).
22. J. Gerl *et al.*, in *Proceedings of the Conference on Physics from Large γ-Ray Detector Arrays, Berkeley 1994* (Laurence Berkeley Laboratory, 1994) Report LBL-35687, vol. **II**, p. 159.
23. M. Wilhelm *et al.*, Nucl. Instrum. Methods in Phys. Res. A **381**, 462 (1996).
24. E. Roeckl *et al.*, Z. Phys. A **294**, 221 (1980).
25. W. Reisdorf, Z. Phys. A **300**, 227 (1981).
26. M.S. Antony *et al.*, At. Data Nucl. Data Tables **66**, 1 (1997).
27. R.P.J. Winsborrow, B.E.F. Macefield, Nucl. Phys. A **182**, 481 (1972).
28. R.B. Schubank *et al.*, Phys. Rev. C **40**, 2310 (1989).
29. A. Poves *et al.*, Nucl. Phys. A **694**, 157 (2001).
30. E. Caurier, computer code ANTOINE, IreS, Strasbourg (1989) unpublished.
31. A.P. Zuker *et al.*, Phys. Rev. C **52**, R1741 (1995).
32. M. Harvey, Adv. Nucl. Phys. **1**, 67 (1968).
33. C.E. Vargas *et al.*, Nucl. Phys. A **690**, 409 (2001).
34. E. Caurier *et al.*, private communication; Phys. Lett. B **522**, 240 (2001).
35. D.J. Dean *et al.*, Phys. Rev. C **59**, 2474 (1999).
36. W.E. Ormand, Phys. Rev. C **55**, 2407 (1997).
37. B.J. Cole, Phys. Rev. C **59**, 726 (1999).
38. P. Möller *et al.*, At. Data Nucl. Data Tables **59**, 185 (1995); **66**, 131 (1997).
39. G.A. Lalazissis *et al.*, Nucl. Phys. A **679**, 481 (2001).
40. M. Hirsch *et al.*, At. Data Nucl. Data Tables **53**, 165 (1993).
41. H. Schatz *et al.*, Phys. Rev. Lett. **86**, 3471 (2001).
42. H. Schatz, private communication, 2001.
43. M.J. López Jiménez *et al.*, *Contribution* to *the International Conference on Physics with Radioactive Ion Beams (ISOL'01), Oak Ridge, 2001.*